

Exploratory Studies of PM₁₀ Receptor and Source Profiling by GC/MS and Principal Component Analysis of Temporally and Spatially Resolved Ambient Samples

Sun Joo Jeon, Henk L.C. Meuzelaar, Sue Anne N. Sheya, JoAnn S. Lighty, Walter M. Jarman, Christian Kasteler, and Adel F. Sarofim
University of Utah, Salt Lake City

Bernd R.T. Simoneit
Oregon State University, Corvallis

ABSTRACT

For a recent exploratory study of particulate matter (PM) compositions, origins, and impacts in the El Paso/Juarez (Paso del Norte) airshed, the authors relied on solvent extraction (SX)-gas chromatography/mass spectrometry (GC/MS) procedures to characterize 24-hr quartz fiber (QF) filter samples obtained from nine spatially distributed high-volume (Hi-Vol) PM₁₀ samplers as well as on thermal desorption (TD)-GC/MS methods to characterize 45 time-resolved (2-hr) filter samples obtained with modified 1-m³/hr PM₁₀ samplers. Principal component analysis and related chemometric techniques were used for data reduction and data fusion as well as for multiway data correlation.

A high degree of correspondence ($R^2 = 0.821$) was found between the rapid TD-GC/MS method (which can

be carried out on 2-hr filter slices containing only microgram amounts of sample) and conventional SX-GC/MS procedures. The four main source patterns of organic PM components observed in GC/MS profiles of both temporally and spatially resolved receptor samples obtained in the El Paso/Juarez border airshed during the study period are interpreted to represent (1) vehicular emissions plus resuspended urban dust; (2) biomass combustion; (3) native vegetation detritus and resuspended agricultural dust; and (4) waste burning. Moreover, principal component analysis of combined, variance-weighted, temporally resolved TD-GC/MS data and spatially resolved SX-GC/MS data was used to determine approximate source locations for specific PM components identified in time-resolved receptor sample profiles. The same approach can be used to determine approximate circadian concentration profiles of specific PM components identified in spatially resolved receptor sample profiles.

IMPLICATIONS

The usefulness of GC/MS techniques for characterizing organic components in ambient PM for the purpose of source characterization and attribution has been demonstrated over the past decade. Yet acceptance of GC/MS techniques in PM receptor modeling studies has been relatively slow, and no standard GC/MS methods for PM source characterization have been approved by the U.S. Environmental Protection Agency. In this study, time-resolved PM receptor profiles obtained by thermal desorption GC/MS analysis of 2-hr quartz filter samples were used and correlated with conventional 24-hr SX-GC/MS data on spatially resolved quartz filter samples by means of principal component analysis. The results provide information about the approximate source location of transient events, as well as about the circadian activity profiles of specific source patterns, thereby enabling rapid, exploratory characterization of PM sources in complex urban environments.

INTRODUCTION

The ability of combined gas chromatography/mass spectrometry (GC/MS) techniques to provide detailed information about the chemical composition and provenance, as well as potential health and environmental impacts, of complex environmental samples has been widely recognized for more than 40 years. Over the past decade or so, many studies have demonstrated the power of GC/MS techniques for particulate matter (PM) source characterization.¹⁻⁹ Yet acceptance of GC/MS techniques in PM receptor modeling studies has been relatively slow, and thus far, no standard GC/MS method for PM source or receptor characterization has been approved by the U.S. Environmental Protection Agency. The El Paso/Juarez region of the U.S./Mexico border has received increasing attention

in recent years because of high air pollution levels in general and PM_{10} levels in particular. The authors performed exploratory chemical analysis of the organic constituents in selected PM_{10} receptor samples from the El Paso/Juarez region airshed using a combination of conventional solvent extraction (SX)-GC/MS procedures as well as a newly developed solvent-free thermal desorption (TD)-GC/MS method.

The solvent-based approach has certain advantages. Several standardized solvent extraction methods which use inexpensive equipment are available, are applicable to many organic as well as several inorganic compound classes, have relatively few matrix effects, and are readily compatible with conventional, high-resolution GC/MS techniques. Extensive source characterization studies of a broad range of organic chemical PM markers in the western U.S. air district have been reported by Rogge¹⁻⁹ and others¹⁰⁻¹⁴ by means of solvent-extraction-based GC/MS techniques.

Although these methods have proven their value in the laboratory for a wide range of applications requiring extraction of soluble analytes from a more or less insoluble matrix, there are several practical problems with the application of solvent-based GC/MS techniques to ambient PM filter sample characterization. Solvent-based GC/MS analysis of filter samples requires relatively large quantities of air PM, typically on the order of 100 mg. The laboratory methods involved are slow and laborious while requiring large quantities of solvents, which have environmental as well as health and safety impacts of their own. Solvent extracts can include significant quantities of large soluble or even polymeric molecules that are unsuitable for direct GC/MS analysis but may contaminate the GC inlet. However, the content of extracted polar compounds (e.g., *n*-alkanoic acids, alkanols, carbohydrates, etc.) can be derivatized for their GC/MS elucidation. In view of these problems, the feasibility of solvent-free techniques for PM filter analysis by GC/MS has been investigated by several authors.¹⁵⁻¹⁸ All solvent-free methods require a certain degree of thermal stimulation, whether based on direct desorption of relatively volatile molecules,¹⁵ pyrolysis of nonvolatile aerosol components,¹⁶⁻¹⁷ or on-line chemical derivatization of highly polar components.¹⁸

The chemical mass balance model has been particularly successful in providing quantitative source contribution estimates among the various receptor-modeling techniques. However, in order to obtain reliable results from mass balance models, strict attention needs to be paid to quantitative measurement of selected source marker compounds and to the identification of all sources concerned.¹⁹⁻²² When using information-rich chromatographic and/or spectrometric

PM characterization methods, the use of principal component analysis (PCA)-based techniques can be highly effective as a tool for receptor modeling.²³ PCA techniques can provide information not only about the minimum intrinsic dimensionality of the independent source patterns involved but also about the degree of correlation between different analytical methods.

The purpose of the work presented here is to demonstrate the power of conventional SX and rapid TD methods to provide detailed information on the composition of complex PM receptor samples collected on spatially and temporally distributed quartz fiber (QF) filters, respectively. Initial visual and MS reference-library-based data analysis is followed by the use of PCA and related chemometric techniques to identify the dominant PM source categories in the El Paso/Juarez border region and to combine the results from the two methods in order to correlate specific time-resolved source patterns with overall source distribution.

EXPERIMENTAL METHODS

Sample Collection

The PM_{10} sampling system used for 2-hr sample collection represents the combination of a standard PM_{10} sampling tower such as that used for dichotomous (dichot) samplers with a single, specially machined QF filter holder, as shown in Figure 1. Sample air was drawn through the filter by use of a small, portable, membrane-type air sampling pump with an attached pressure gauge. The air stream, at a flow rate of 16.7 L/min, was directed onto two stacked (primary and backup) 21-mm-diameter QF filters, which were supported by a stainless steel screen. Filters were changed every 2 hr. For PM_{10} collection methods for MS investigation, QF filters were selected because of their inherent low background and high chemical inertness as well as excellent thermal stability and high collection efficiency. Filter sheets were cut into 21-mm-diameter disks that were then cleaned by baking in a covered porcelain crucible at 725 °C for 12–24 hr to remove any adsorbed organic material.

Standard high-volume (Hi-Vol) PM_{10} samplers (1 m³/min) were used for 24-hr sample collection of PM_{10} by filtration of the ambient air using QF filters (20 × 25 cm² surface) that were annealed for 3 hr at 560 °C prior to sampling. Hi-Vol samplers for 24-hr sample collection were set up in nine spatially distributed locations in the El Paso/Juarez border region, and the special time-series samplers were used at four different sites (Sun Metro, Sodar, Techschool, and Juarez Police Station), as shown in Figure 2. The Sun Metro and Techschool sites were designed to coincide with two of the Hi-Vol sites. Table 1 summarizes the data sets of sampling sites for spatially and temporally resolved PM samples used for data handling.

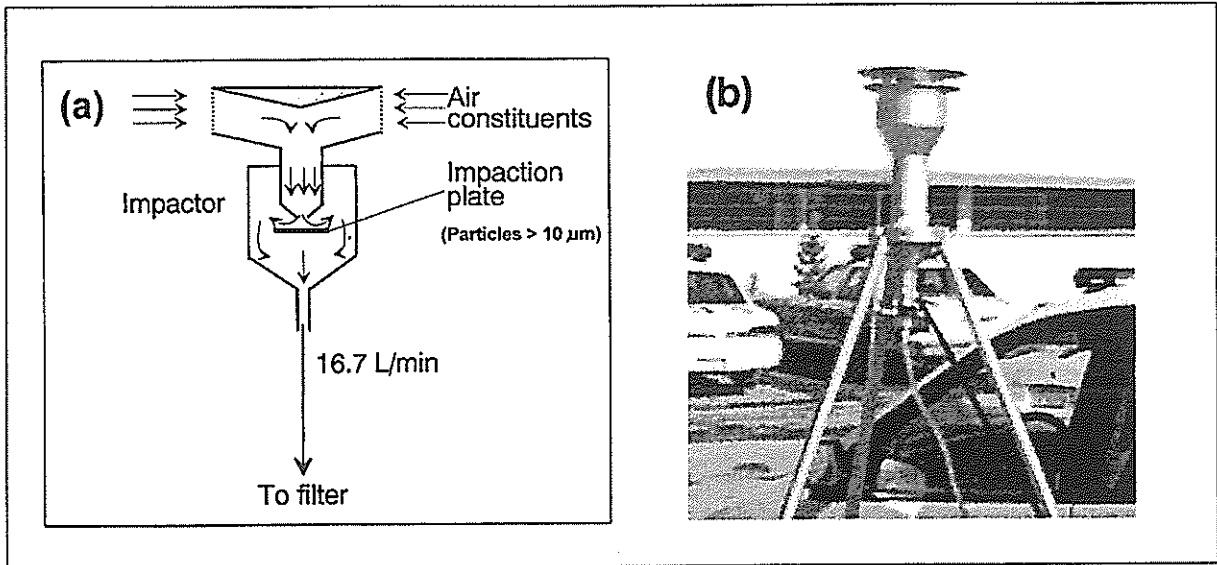


Figure 1. Sample collection system used for collection of PM₁₀ of 2-hr time-resolved data: (a) schematic diagram of the dichot inlet to accommodate a 21-mm-diameter QF filter; and (b) photograph of the dichot sampling tower on top of the tripod.

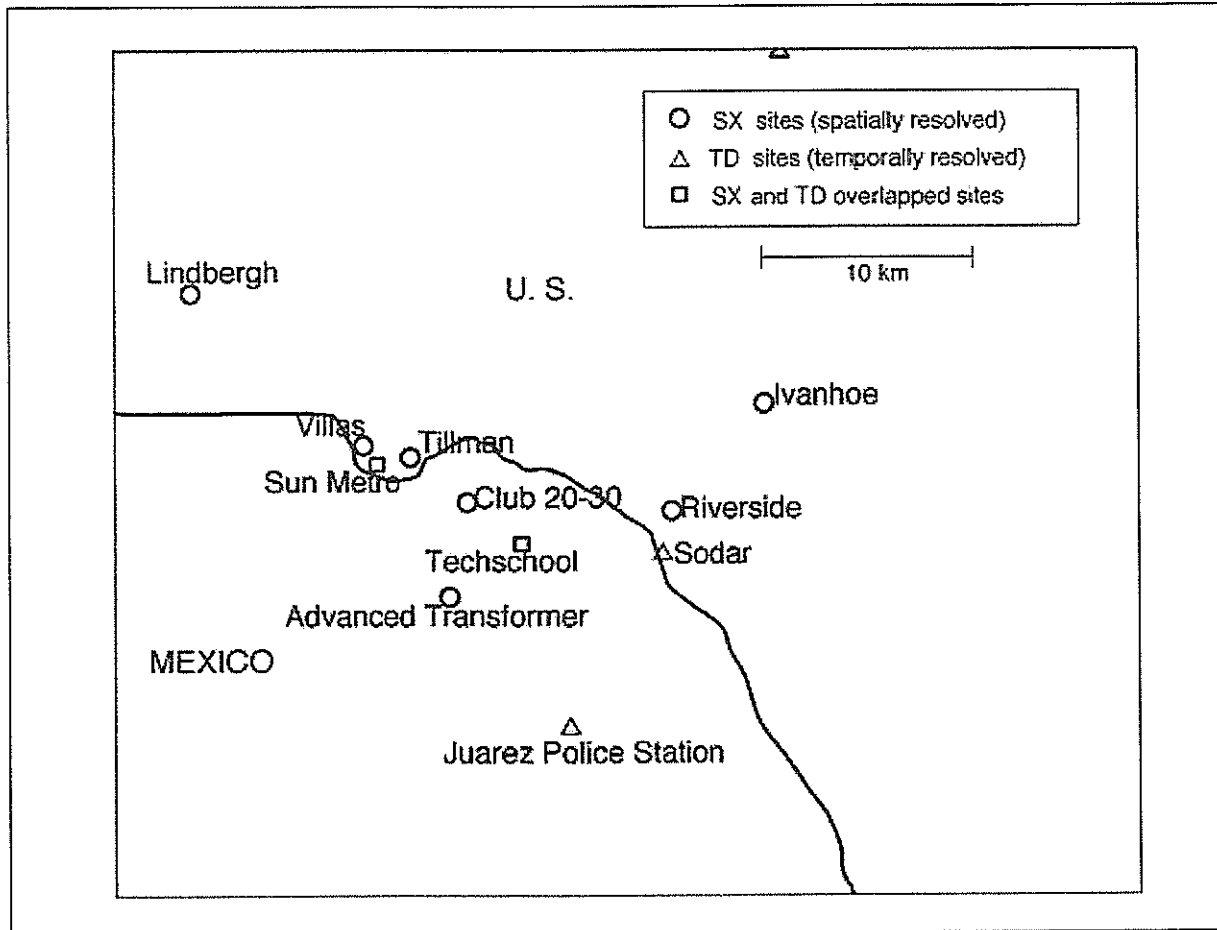


Figure 2. El Paso/Juarez satellite map around the U.S./Mexico border showing the locations for collection of PM for nine spatial samples for SX-GC/MS analysis, four temporal samples for TD-GC/MS analysis, and two overlapped sites.

Table 1. Data sets of sampling sites for collection of particles along the U.S./Mexico border analyzed using GC/MS.

Sampling Site	Date	Sampling Time	
Space-Resolved Data Sets for SX-GC/MS			
Lindbergh	12/03/98, Thursday	24 hr	
Riverside	12/03/98	24 hr	
Villas	12/03/98	24 hr	
Ivanhoe	12/03/98	24 hr	
Sun Metro	12/03/98	24 hr	
Advanced Transformer	12/03/98	24 hr	
Tillman	12/03/98	24 hr	
Club 20-30	12/03/98	24 hr	
Techschool	12/03/98	24 hr	
Time-Resolved Data Sets for TD-GC/MS			
Sun Metro and Techschool	12/03/98, Thursday	12:00–2:00 p.m.	
	12/03/98	2:00–4:00 p.m.	
	12/03/98	4:00–6:00 p.m.	
	12/03/98	6:00–8:00 p.m.	
	12/03/98	8:00–10:00 p.m.	
	12/03/98	10:00 p.m.–12:00 a.m.	
	12/04/98, Friday	12:00–2:00 a.m.	
	12/04/98	2:00–4:00 a.m.	
	12/04/98	4:00–6:00 a.m.	
	12/04/98	6:00–8:00 a.m.	
	12/04/98	8:00–10:00 a.m.	
	Sodar and Juarez Police Station	12/04/98	12:00–2:00 p.m.
		12/04/98	2:00–4:00 p.m.
		12/04/98	4:00–6:00 p.m.
12/04/98		6:00–8:00 p.m.	
12/04/98		8:00–10:00 p.m.	
12/04/98		10:00 p.m.–12:00 a.m.	
12/05/98, Saturday		12:00–2:00 a.m.	
12/05/98		2:00–4:00 a.m.	
12/05/98		4:00–6:00 a.m.	
12/05/98		6:00–8:00 a.m.	
12/05/98	8:00–10:00 a.m.		
12/05/98	10:00–12:00 a.m.		

Particle and Meteorology Measurements

In addition to collection of PM of filters for chemical analysis at the Sun Metro and Sodar sites, particle size distribution measurements in the 0.3–10 μm diameter size range using an 8-size multichannel particle counter were performed at 4-min intervals. Relative particle volumes were calculated from the particle counter data assuming spherical shape. At the Sun Metro site, β -gauge measurements were performed, and a strong linear correlation ($R^2 = 0.923$) between particle volume and β -gauge reading ($\mu\text{g}/\text{m}^3$) was found. Therefore, PM concentrations were calculated from the linear relationship between particle volume and β -gauge reading without the need to perform weight/volume calculations of particle data. Meteorological parameters

of temperature, inversion height, wind speed, and wind direction were obtained from a Sodar system operated by the TNRCC (Texas Natural Resource Conservation Commission).

Sample Preparation and Introduction

Figure 3 shows the process of sample preparation and introduction for TD-GC/MS. The TD method was applied to analyze the 2-hr sampling filters and begins with cutting $1.5 \times 18\text{-mm}^2$ strips from the filters, which represents ~10% of the exposed sample area as shown in Figure 3b. A homemade strip cutter consisting of parallel razor blades and a pair of forceps cleaned by ultrasonication in methanol and dichloromethane were used to cut the filter strips while avoiding contamination. The filter strips were then positioned inside a special glass reaction tube that was lined with a ferromagnetic foil characterized by the Curie-point temperature of 315 $^\circ\text{C}$ for desorption, and placed into a Curie-point desorption reactor for desorption of volatile and semivolatile organic compounds. A more detailed representation of the GC inlet for the Curie-point thermal desorption unit¹⁵ is shown in Figure 3d. In the Curie-point-type desorption, a high-frequency induction coil surrounds the glass tube and heats the foil by induction. The foil is heated until its Curie point (the temperature at which the wire becomes paramagnetic, and its energy intake drops, thus holding the temperature of the foil at this point) is reached. Flash desorption of organic compounds from the ambient particles immobilized by the QF filter strips is achieved using a total heating time of 10 sec under a continuous flow of He carrier. This continuous flow of He transfers the analytes from the reaction zone into a fused silica capillary column of a GC, coupled to an MS.

Filters from a 24-hr Hi-Vol sampler were mainly prepared by the SX method and partly used for the TD method in the case of need for comparison between SX and TD methods. Immediately after sampling, the filters were stored in a freezer at $-20\text{ }^\circ\text{C}$ until extraction. An extraction protocol designed for the analysis of trace amounts of organic compounds found in PM was followed. The method is described extensively elsewhere.^{1,14} In brief, each filter composite with 13-cm^2 sections was spiked prior to extraction with known amounts of perdeuterated tetracosane ($n\text{-C}_{24}\text{D}_{50}$), which served as an internal standard. The sample was extracted 3 times with dichloromethane:methanol (4:1) and then filtered with a vacuum system through a teflon filter. After this, the extracts were combined and the extract volume was reduced to 1 mL on a Rotavapor system. Two microliters of aliquot were injected into the GC/MS system, and one other aliquot of the extract was derivatized by adding bis(trimethylsilyl)trifluoroacetamide to

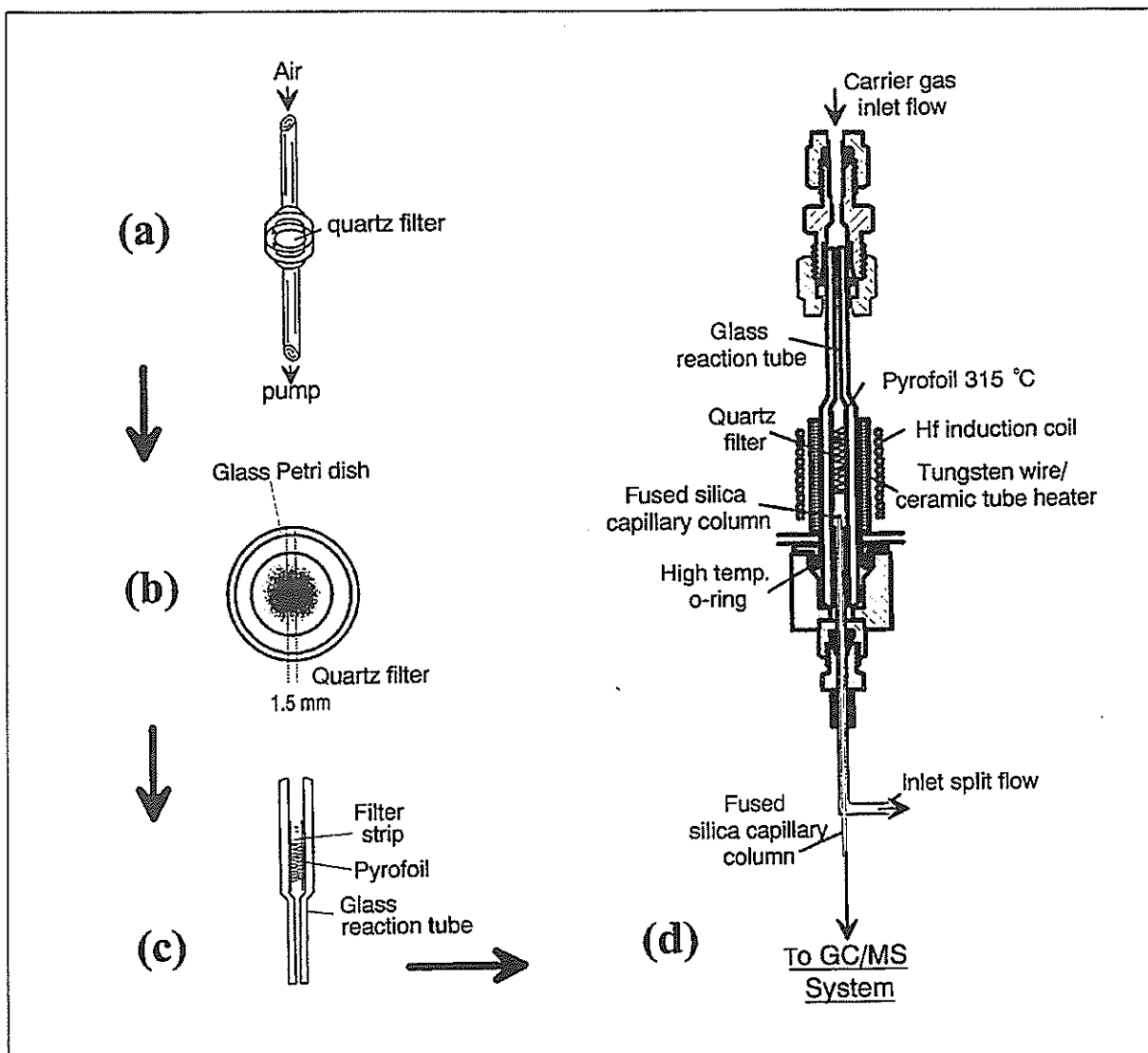


Figure 3. Diagram of sample preparation and introduction for the TD-GC/MS system: (a) particle collection on the filter; (b) filter cut as a small strip (1.5 × 18 mm²) for insertion into glass tube; (c) filter strip positioning inside the glass tube lined with a ferromagnetic foil that has a Curie-point temperature of 315 °C for desorption; and (d) detailed configuration of the Curie-point thermal desorption unit used for vaporization of volatile and semivolatile organic compounds into the GC/MS system.

convert organic acids to their trimethylsilyl ester analogues and to convert other compounds having active H atoms (e.g., alkanols, phenols) to their trimethylsilyl ethers.

GC/MS Analysis

Subsequent to sample desorption and introduction of compounds through a Curie-point thermal desorption unit into a fused silica capillary column, a temperature-programmed separation of analytes coupled with simultaneous MS monitoring was initialized. The GC analysis for the TD method was carried out on a Hewlett-Packard (HP) Model 5890 gas chromatograph using an HP-5MS

column with a 25-m-long, 0.20-mm-i.d. fused silica capillary coated with a 0.33- μ m-thick film equipped with a thermal desorption inlet. An HP Model 6890 GC with a conventional injection port was used for the analysis of liquid sample from the SX method by a DB-5MS (J & W Scientific) column with a 60-m-long, 0.25-mm-i.d. fused silica capillary coated with a 0.25- μ m-thick film. The oven was temperature-programmed from 50 to 320 °C at a rate of 3–15 °C/min.

Compound identification and peak area integration were conducted using quadrupole-type Mass Selective Detectors (MSD 5972 or MSD 5973 from HP) operated in the electron impact mode with an electron energy of 70 eV.

A group of target compounds were identified by an initial qualitative analysis of representative GC/MS runs from the data file with the highest peak in each TD sampling site. Selected ion chromatograms of indicative m/z ratios from these potential compounds of interest were used to obtain retention times and the relative intensity of target compounds.

Multivariate Data Analysis Techniques

Data were reduced, interpreted, and evaluated with the technique of multivariate data analysis.²⁴ Multivariate data analysis techniques used are primarily based on an exploratory PCA data analysis approach with subsequent orthogonal rotation of the PCA components using the Varimax technique. PCA is a data analysis tool that is used to reduce the dimensionality of a large number of interrelated variables while retaining as much of the information (variance) as possible. PCA calculates a noncorrelated set of variables ("factors" or "components") that are ordered so the first few retain most of the variance present in the original variables. The first step in PCA is usually to create an autoscaled data matrix by subtracting the variable mean and dividing by the standard deviation. A commercially available NCSS statistical software package was used to perform PCA in this study.

Several methods have been proposed for determining the number of factors that should be kept for further analysis. The scree plot, a plot of factors versus eigenvalues, is a graphical approach for determining the number of factors. Usually factors with eigenvalues of <1 are discarded.²⁵ However, important information about possible outliers and linear dependencies may sometimes be determined from the factors associated with relatively small eigenvalues, so these may need to be investigated as well. Another approach is to use the first "break" in the slope of the scree curve when following the curve in downward or, rather, in upward direction. This last method was used in our data sets.

In the Varimax rotation technique,²⁶ the axes are rotated to maximize the sum of the variances of the squared loadings (correlations) within each column of the loadings matrix. Maximizing according to this criterion forces the loadings to be either large or small. In our data sets, Varimax rotation is applied to highlight components or trends in factor space that are each highly correlated with at least several of the original variables. This approach reduces the tendency to produce a single dominant component and makes the variances of the components more equal. This simplifies the interpretation of the factor to a consideration of a few variables that are often more readily identifiable as specific source components.

RESULTS AND DISCUSSIONS

Physical Measurements

Particle concentration data and meteorological parameters shown in Figure 4 illustrate the low PM pollution levels at the start of the 48-hr monitoring window. This was due to unseasonably intense and prolonged periods of rainfall throughout the previous two days, which, in fact, delayed the start of the monitoring window—originally planned for 72 hr—by nearly a day. During the remaining 48 hr, average particle concentrations shown in Figures 4a–c, as calculated from multichannel particle data by correlation with β -gauge readings at the Sun Metro site, were seen to increase after the rainfall as the prevailing winds (in Figure 4h) gradually decreased and inversion height (in Figure 4e) came to a low on the night of December 4. Concentration of the smaller particles of $PM_{2.5}$ rises faster than that of PM_{10} . Also, daily temperatures (in Figure 4d) resumed their normal circadian rhythm, accompanied by characteristic changes in inversion layer height (in Figure 4e), as determined from the Sodar readings.

The gradually increasing PM concentration, interspersed by rush hour traffic peaks, culminated in the severe transient PM episode in the late evening of December 4, when PM_{10} concentration reached values in the several hundred- $\mu\text{g}/\text{m}^3$ range. Much remains to be learned about these types of late-night PM episodes, which in this case apparently represented transport of massive dust clouds accumulated over the city of Juarez to the American side by little or no wind, cooling temperatures, and low inversion ceilings. However, such episodes appear to be relatively frequent at the U.S./Mexico border, particularly in the vicinity of the largest Mexican border cities. Over a total of 10–12 monitored winter periods, 3–4 severe, late-evening PM events were observed at various U.S. border sites,²⁷ including Calexico (vicinity of Mexicali; $>600 \mu\text{g}/\text{m}^3$), Hidalgo (vicinity of Reynosa; $>1000 \mu\text{g}/\text{m}^3$), Brownsville (vicinity of Matamoros; $>200 \mu\text{g}/\text{m}^3$), and the above-mentioned Sodar site (vicinity of Juarez; $>250 \mu\text{g}/\text{m}^3$). Because of their transient nature, the effect of these nocturnal episodes on overall PM compliance, and possibly on human health, appears to have been insufficiently recognized.

TD-GC/MS Analysis

Currently, the TD-GC/MS appears to be the only GC/MS method capable of characterizing organic adsorbates on 2-hr filter samples because of the few microgram quantities of PM present on a typical strip of filter material obtained within such a relatively short time. To evaluate the performance of the novel TD-GC/MS method, the authors briefly evaluated the contribution of background

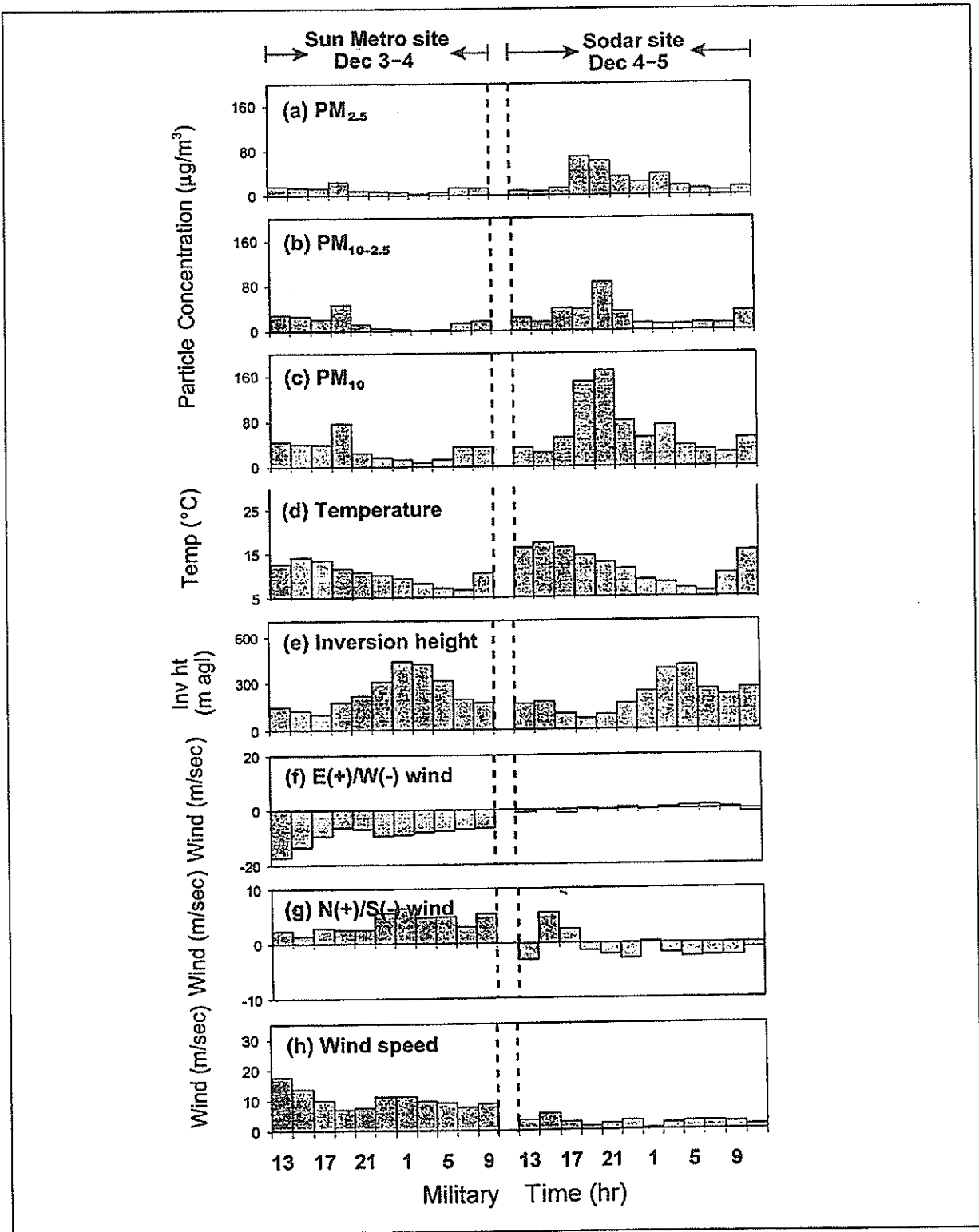


Figure 4. Particle concentration and meteorological data for the Sun Metro and Sodar sites: (a-c) Particle concentration profiles calculated from an 8-channel, size-distributed particle counter by correlation with β -gauge readings; (d) ambient temperature profile; (e) inversion height profile; (f) east/west wind vector; (g) north/south wind vector; and (h) wind speed calculated from (f) and (g). Figures 4d-h were provided by the TNRC Sodar system; $PM_{10-2.5}$ means the particle size was between 2.5 and 10 μm .

signals and the reproducibility of replicate analyses. Representative background signal levels from a strip of cleaned filter analyzed by TD-GC/MS are shown in Figure 5. Comparison with the signal levels shown in Figure 8a reveals that residual background signals from the filter contribute no more than a few percent to the signal intensities observed from the filters loaded with ambient PM. Moreover, it should be kept in mind that the subsequent PCA performed on all the data is quite effective in removing background patterns that do not correlate with the spatial and temporal variations of the ambient PM compounds but are either more or less constant or else tend to fluctuate in a random manner.

The repeatability of TD-GC/MS analysis was investigated in Figure 6 using the plots of the peak intensities obtained from two replicate runs of ambient sample filter under the same experimental conditions. It was found that *n*-alkanoic acids tend to deviate more than other PM adsorbate compound classes, as evident in Figure 6, apparently as a result of their highly polar and/or thermally labile nature. The accuracy of the TD-GC/MS results was not measured in this study, but similar results were recently reported by Waterman et al.²⁸ They measured the polycyclic aromatic hydrocarbon (PAH) concentrations of PM in an Urban Dust standard reference material using a TD-GC/MS instrument equipped with a desorption liner, and found a relative error of 12% in the quantification of eight different PAHs in the 178–252 MW range.

Examples of TD-GC/MS analysis results on 2-hr QF filter samples loaded with microgram quantities of PM are shown in Figure 7 and Figure 8a. The selected,

time-resolved compound profiles in Figure 7 reveal several chemical events and trends, generally reaching their highest maxima during the high, nocturnal PM episode on December 4 (Friday). Each profile has been selected to represent an entire suite of compounds (e.g., *n*-alkanes, hopanes, *n*-alkanoic acid, amyriins, PAHs, phenols, and resin acids), as listed in Table 2. Each of the 91 compounds in Table 2 was identified and quantified through peak area integration in every TD-GC/MS run. The total ion chromatogram (TIC) profile and a few selected ion chromatogram profiles from a single TD-GC/MS run are shown in Figure 8a. They reveal a complex pattern of GC peaks superimposed on a broad “unresolved complex mixture” (UCM) of branched and cyclic compounds seen in nearly all GC/MS data on ambient PM samples and thought to largely represent the complex mixtures of isomeric hydrocarbon compounds emitted by a variety of incomplete combustion processes (e.g., lubrication oils from engine exhaust).

Much of the literature on GC/MS analysis of organic compounds in PM produced by sources derives from the work of Rogge et al.,^{1,9} who performed systematic SX-GC/MS analyses on PM filter samples collected from a wide range of different emissions. The SX-GC/MS literature data, together with a vast body of literature data on pyrolysis products from biomass, fossil fuels, geochemical markers, humic substances, plastics, and rubber emitted during smoldering combustion or other incomplete combustion processes, enable us to make tentative source assignments for quite a few of the organic substances found in PM and released by thermal desorption, such as PM “adsorbates”.

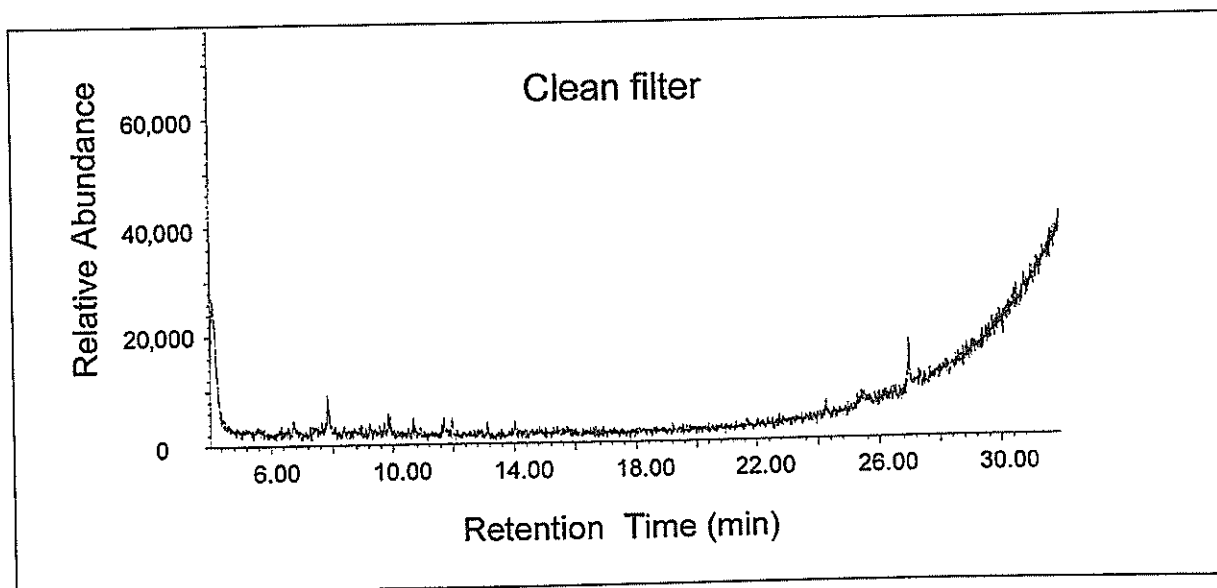


Figure 5. Total ion chromatogram obtained by TD-GC/MS analysis of a clean filter. Compare the residual background peak with TIC intensities of PM-loaded filter samples in Figure 8a.

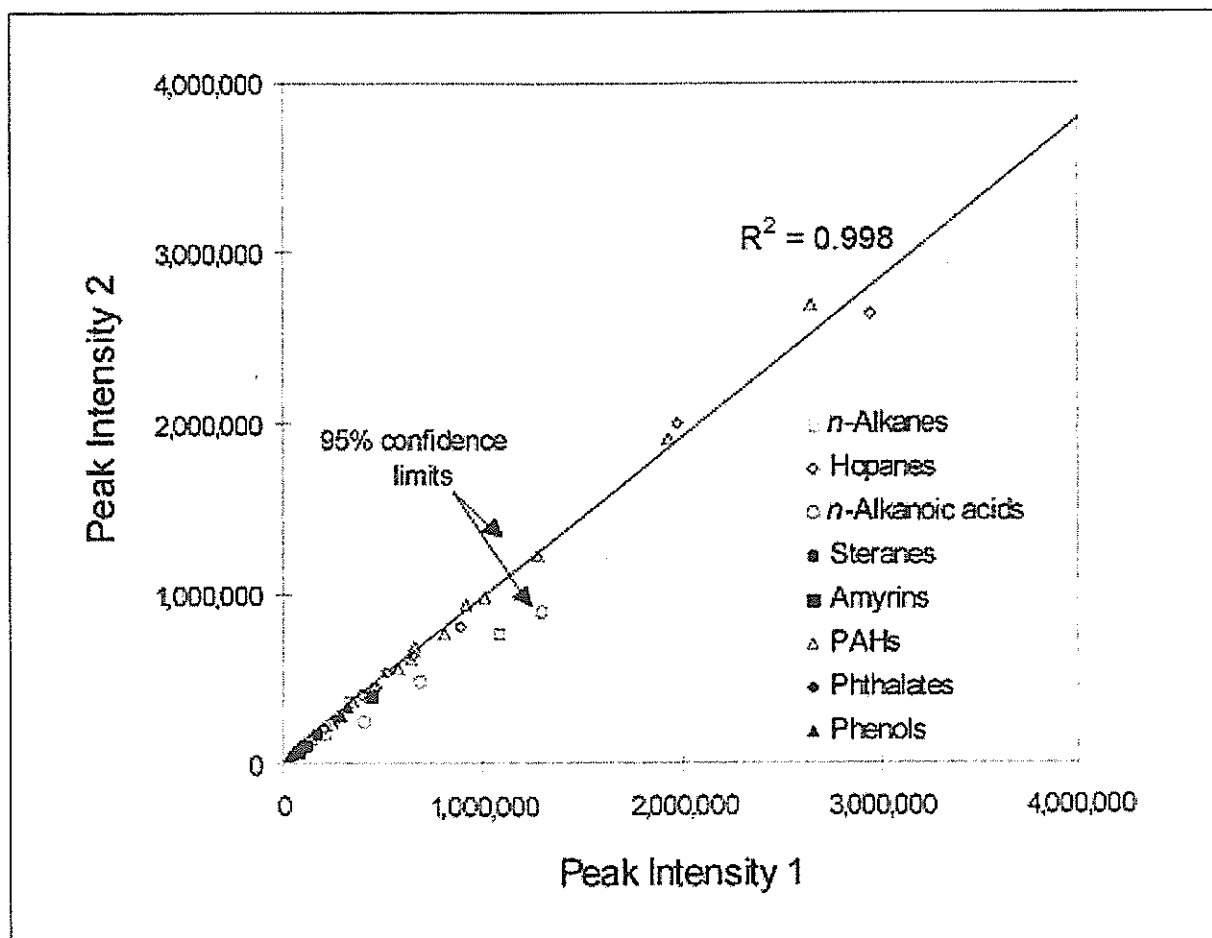


Figure 6. Correlation of TD-GC/MS peak intensities obtained from two replicate runs of an ambient sample filter collected at the Techscho ol site.

An important question, of course, is whether the PM components observed by TD-GC/MS differ substantially from the components observed by SX-GC/MS.

Comparison of TD-GC/MS and SX-GC/MS Data

Figures 8a and 8b provide a side-by-side visual comparison of the GC/MS profiles produced when applying the two different methods to samples obtained from a single 24-hr, Hi-Vol QF filter obtained at the Techschool site. Figure 8a was obtained by insertion of a small Hi-Vol filter strip directly into the Curie-point thermal desorption unit, and Figure 8b was obtained by depositing a small aliquot of the solvent extract from the same filter on a clean filter substrate and then heating with same Curie-point device. Although the solvent extraction method can be expected to liberate a broader range of compounds of different molecular size from the filter, in view of the fact that even many polymeric compounds are known to be soluble, only those compounds volatile enough to elute from the chromatographic column are detected in either case.

Figure 9 shows the plots of the integrated areas for the selected ions used in Figure 8 so as to enable a quantitative comparison between the SX and TD methods. A good correspondence ($R^2 = 0.821$) was found between the two methods when all of the compound classes included were accounted for by a single linear fit. Even better linear fits were found for each class of compounds (i.e., $R^2 = 0.975$ for *n*-alkanes, $R^2 = 0.998$ for hopanes and steranes, $R^2 = 0.731$ for *n*-alkanoic acids, $R^2 = 0.978$ for PAHs, and $R^2 = 0.940$ for phenols). Again, however, *n*-alkanoic acids provided the lowest fit ($R^2 = 0.731$). However, it should be kept in mind that for solvent-extract-based GC/MS methods, *n*-alkanoic acids were determined after derivatization, thereby introducing one more source of variance.

From Figures 8 and 9, the high degree of similarity between the two methods is explained, particularly when comparing the chemical compound classes and their relative intensities on either side. At first view, the TIC profiles in Figure 8 appear to differ markedly, especially with regard to the early eluting compound suites and the relative proportions of the UCM maxima. However, it should

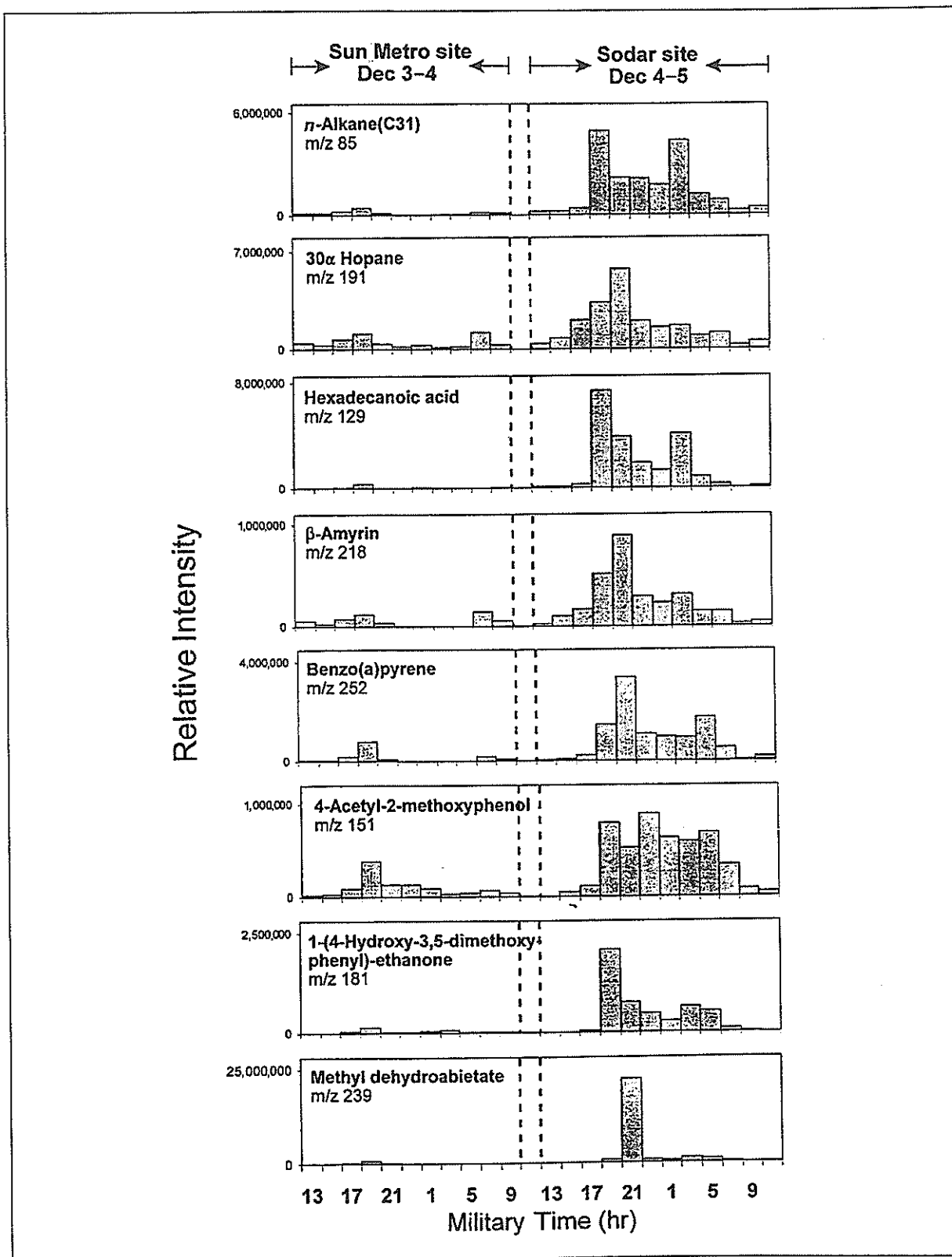


Figure 7. Time-resolved receptor profiles of eight selected organic PM components obtained from the TD-GC/MS analysis as represented by specific key ion intensity.

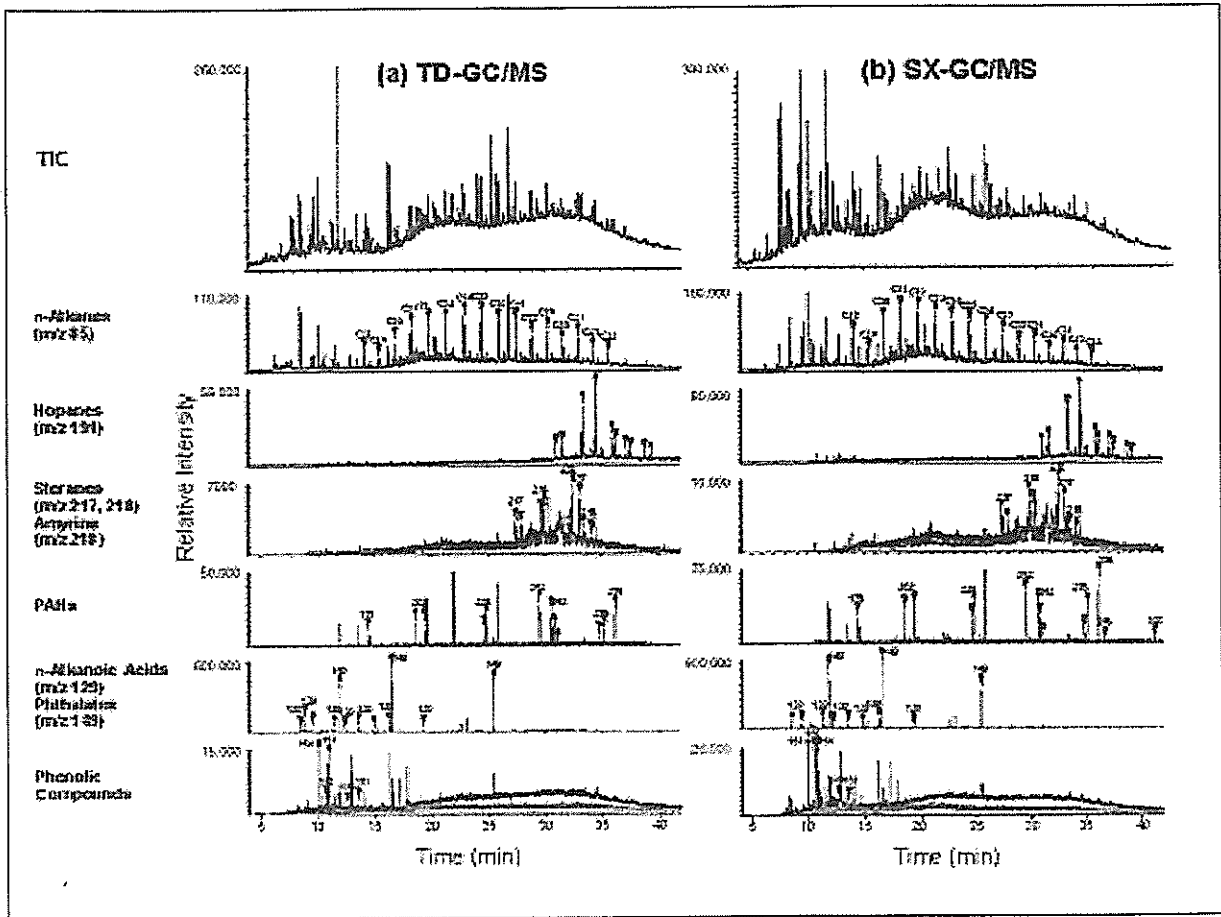


Figure 8. Comparison of TD-GC/MS and SX-GC/MS profiles using TICs and ion chromatograms obtained from the same Hi-Vol QF filter collected at the Techschool site: (a) profiles from direct insertion of filter strip and Curie-point heating to 315 °C; and (b) profiles from depositing a 1-mL aliquot of solvent extract into the same Curie-point device.

be pointed out that the TD-GC/MS analysis was performed on a small section of unextracted filter material several months after the bulk of the filter material had been solvent-extracted. Clearly, some of the more volatile compounds, whether appearing as resolved or unresolved GC peaks, can be expected to be lost. Indeed, the last eluting one-third of each of the two TIC profiles, assumed to represent the PM components with lowest relative volatility, are virtually indistinguishable.

This hypothesis is further supported by a more careful comparison of the two UCM profiles, represented as *m/z* 95 (for naphthenes)¹⁴ in Figure 10. With the exception of the earliest GC peaks, presumably affected by some residual QF filter background signals and by the isothermal starting plateau in the temperature program of the GC oven, the difference in relative UCM intensities between the TD-GC/MS and SX-GC/MS profiles appears to correlate smoothly with the average boiling points of the compounds involved, considering the DB-5 or HP-5 columns used, which have almost nonpolar stationary phase

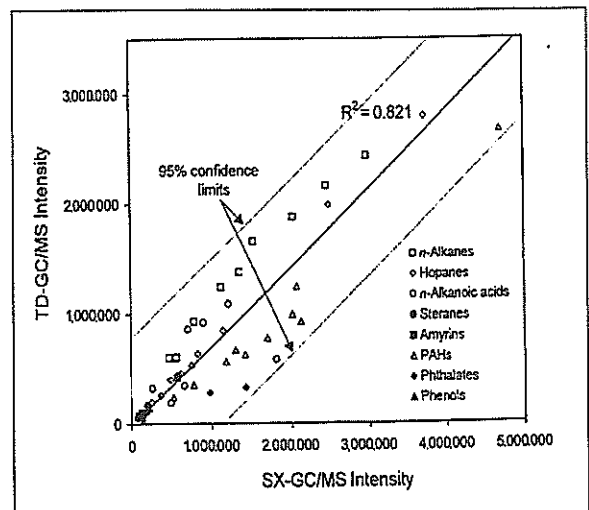


Figure 9. Direct comparison of measured TD-GC/MS and SX-GC/MS peak intensities using integrated peak areas from the ion chromatograms shown in Figure 8. The data points represent the average values of two replicate runs.

Table 2. List of organic compounds identified from PM₁₀ in the El Paso/Juarez airshed and factor loadings for the combined data matrix of temporally and spatially resolved GC/MS data^a after Varimax rotation.

Compounds	Factor 1	Factor 2	Factor 3	Factor 4
<i>n</i>-Alkanes				
<i>n</i> -Octadecane	0.02	-0.77	0.11	-0.01
<i>n</i> -Nonadecane	0.07	-0.14	0.06	0.05
<i>n</i> -Eicosane	0.27	-0.18	-0.16	0.03
<i>n</i> -Heneicosane	0.10	<u>-0.56</u>	0.07	0.02
<i>n</i> -Docosane	<u>-0.50</u>	<u>-0.66</u>	0.16	-0.01
<i>n</i> -Tricosane	<u>-0.59</u>	-0.15	<i>0.76</i>	-0.12
<i>n</i> -Tetracosane	-0.03	0.00	<i>0.73</i>	0.02
<i>n</i> -Pentacosane	<u>-0.54</u>	0.00	0.81	-0.15
<i>n</i> -Hexacosane	<u>-0.43</u>	-0.00	0.87	-0.18
<i>n</i> -Heptacosane	<u>-0.43</u>	0.00	0.87	-0.18
<i>n</i> -Octacosane	<u>-0.41</u>	0.00	0.88	-0.12
<i>n</i> -Nonacosane	<u>-0.42</u>	0.00	0.89	-0.14
<i>n</i> -Triacontane	<u>-0.44</u>	-0.00	0.87	-0.09
<i>n</i> -Hentriacontane	<u>-0.48</u>	-0.03	0.85	-0.11
<i>n</i> -Dotriacontane	<u>-0.42</u>	-0.03	0.90	-0.02
<i>n</i> -Tritriacontane	<u>-0.46</u>	-0.04	0.87	-0.04
Hopanes				
22,29,30-trisnorhopane	-0.90	0.06	0.35	-0.10
22,29,30-trisnorhopane	-0.87	0.07	0.39	-0.10
17 α (H),21 β (H)-29-norhopane	-0.93	0.03	0.29	-0.11
17 α (H),21 β (H)-hopane	-0.92	0.05	0.31	-0.09
17 β (H),21 β (H)-hopane	-0.91	0.08	0.34	-0.10
17 β (H),21 α (H)-hopane	-0.91	0.07	0.36	-0.11
(22S)-17 α (H),21 β (H)-30-homohopane	-0.91	0.07	0.34	-0.09
(22R)-17 α (H),21 β (H)-30-homohopane	-0.92	0.06	0.33	-0.06
(22S)-17 α (H),21 β (H)-30-bishomohopane	-0.93	-0.00	0.32	-0.06
(22R)-17 α (H),21 β (H)-30-bishomohopane	-0.91	-0.02	0.32	-0.06
<i>n</i>-Alkanoic Acids				
Nonanoic acid	0.12	-0.95	-0.15	-0.00
Decanoic acid	0.05	<i>-0.78</i>	-0.04	-0.12
Dodecanoic acid	-0.13	-0.85	-0.01	-0.25
Tridecanoic acid	0.10	-0.94	-0.11	-0.05
Tetradecanoic acid	-0.16	-0.94	0.13	-0.17
Pentadecanoic acid	0.04	-0.97	0.01	-0.08
Hexadecanoic acid	-0.15	-0.91	0.29	-0.07
Octadecanoic acid	0.12	-0.93	-0.16	-0.13
Steranes				
20S-13 β (H),17 α (H) diacholestene	-0.92	-0.06	0.34	-0.11
20R-13 β (H),17 α (H) diacholestene	-0.95	-0.07	0.24	-0.10
20R-24R-5 α (H),14 α (H),17 α (H) ethylcholestane	-0.89	0.02	0.43	-0.11
20R-5 α (H),14 β (H),17 β (H) cholestane	-0.96	-0.15	0.16	-0.10
20S-5 α (H),14 β (H),17 β (H) cholestane	-0.93	-0.07	0.33	-0.09
Amyrins				
β -Amyrin	-0.86	0.11	0.41	-0.04

Note: Bold, italic, and underlined characters represent loadings with values higher than 0.80, between 0.60 and 0.80, and between 0.40 and 0.60, respectively. ^aNine spatially resolved data and 11 time-resolved data for the Sun Metro site and 12 time-resolved data for the Sodar site were used.

Table 2. (cont.) List of organic compounds identified from PM₁₀ in the El Paso/Juarez airshed and factor loadings for the combined data matrix of temporally and spatially resolved GC/MS data^a after Varimax rotation.

Compounds	Factor 1	Factor 2	Factor 3	Factor 4
α -Amyrin	-0.14	-0.07	<i>0.73</i>	0.01
α -Amyrin acetate	-0.32	-0.05	<i>0.74</i>	-0.01
PAHs and Aromatics				
Phenanthrene	<i>-0.73</i>	0.22	<i>0.45</i>	0.07
Fluoranthene	<i>-0.64</i>	-0.12	0.18	-0.03
Pyrene	<i>-0.73</i>	-0.11	0.35	-0.04
Retene	<i>-0.60</i>	0.34	0.37	0.07
Benzo[ghi]perylene	<i>-0.84</i>	-0.05	0.23	-0.06
Chrysene	<i>-0.83</i>	-0.03	0.27	-0.08
Benzo[ghi]fluoranthene	<i>-0.88</i>	-0.03	0.20	-0.11
Benzo[e]pyrene	<i>-0.90</i>	-0.11	0.24	-0.12
Benzo[a]pyrene	<i>-0.90</i>	-0.02	0.26	-0.10
Perylene	<i>-0.92</i>	-0.03	0.29	-0.08
Indeno[1,2,3-cd]pyrene	<i>-0.91</i>	-0.20	0.16	-0.15
Indeno[1,2,3-cd]fluoranthene	<i>-0.88</i>	-0.28	0.11	-0.15
Benzo[ghi]perylene	<i>-0.91</i>	-0.30	0.11	-0.18
Dibenzo[def,mno]chrysene	<i>-0.96</i>	-0.03	0.20	-0.11
Dibenzopyrene1	<i>-0.80</i>	<i>-0.44</i>	0.09	-0.07
Dibenzopyrene2	<i>-0.58</i>	<i>-0.57</i>	-0.13	-0.09
Dibenzopyrene3	<i>-0.66</i>	<i>-0.49</i>	-0.15	-0.09
Phthalates				
Diethyl phthalate	-0.25	-0.30	0.16	<i>-0.82</i>
Dibutyl phthalate	<i>-0.55</i>	0.08	<i>0.65</i>	-0.35
Bis-(2-ethylhexyl)phthalate	-0.12	0.33	0.39	-0.00
Aliphatic Alcohols and Phenols				
2-(2-butoxyethoxy)ethanol	-0.19	<i>-0.69</i>	0.01	<i>-0.60</i>
2-(2-(2-methoxyethoxy)ethoxy)ethanol	-0.05	<i>-0.66</i>	-0.05	0.01
2-Methyl-2,2-dimethyl-1-(2-hydroxy-1-methylethyl)propyl propanoate	-0.05	-0.35	0.12	<i>-0.71</i>
2-Methyl-3-hydroxy-2,4,4-trimethylpentyl propanoate	-0.17	-0.18	0.23	<i>-0.77</i>
4-Hydroxy-3-methoxybenzaldehyde	<i>-0.40</i>	0.33	0.33	-0.06
1-(2-hydroxy-3-methoxy-4-methylphenyl)-ethanone	-0.22	<i>-0.42</i>	0.37	<i>-0.67</i>
4-Acetyl-2-methoxyphenol	<i>-0.44</i>	0.09	<i>0.48</i>	-0.24
4-Hydroxy-3,5-dimethoxybenzaldehyde	<i>-0.62</i>	0.00	<i>0.63</i>	-0.16
1-(4-hydroxy-3,5-dimethoxyphenyl)-ethanone	<i>-0.48</i>	-0.01	<i>0.76</i>	-0.01
N-Containing				
1-Methyl-2-pyrrolidinone	0.04	0.26	0.02	-0.00
Quinoline	0.15	<i>0.46</i>	-0.14	0.19
Isoquinoline	-0.34	0.09	0.09	-0.30
N,N-dibutylformamide	-0.21	-0.35	0.06	<i>-0.67</i>
Other O-Containing				
Nonanal	0.11	<i>0.45</i>	0.07	0.16
3-Hexen-2-one	0.07	-0.33	-0.12	<i>-0.52</i>
Bis(2-butoxyethyl) ether	-0.36	-0.27	0.28	<i>-0.67</i>
Trimethylbenzaldehyde	-0.24	0.02	<i>0.40</i>	<i>-0.52</i>

Note: Bold, italic, and underlined characters represent loadings with values higher than 0.80, between 0.60 and 0.80, and between 0.40 and 0.60, respectively. ^aNine spatially resolved data and 11 time-resolved data for the Sun Metro site and 12 time-resolved data for the Sodar site were used.

Table 2. (cont.) List of organic compounds identified from PM₁₀ in the El Paso/Juarez airshed and factor loadings for the combined data matrix of temporally and spatially resolved GC/MS data^a after Varimax rotation.

Compounds	Factor 1	Factor 2	Factor 3	Factor 4
5,6,7,7a-tetrahydro-4,4,7a-trimethyl-2(4H)-benzofuranone	-0.36	0.23	0.45	-0.40
2-Methyl-1-(1,1-dimethylethyl)-2-methyl-1,3-propanediyl Propanoate	-0.69	0.00	0.35	-0.50
Tetradecanal	0.14	-0.41	-0.02	-0.13
Methyl tetradecanoate	-0.04	0.04	0.02	0.07
6,10,14-trimethyl-2-pentadecanone	-0.42	0.05	0.62	-0.33
1H-phenalen-1-one	-0.76	-0.01	0.34	-0.14
Isopropyl hexadecanoate	-0.41	0.28	0.12	-0.20
9,10-Anthracenedione	-0.67	0.06	0.38	-0.22
Methyl dehydroabietate	-0.94	-0.02	-0.10	0.07
Other Compounds				
Benzoic acid	-0.23	-0.86	0.06	-0.27
Tri-n-butylphosphate	-0.04	-0.32	-0.01	-0.09
Quaterphenyl	-0.52	0.08	0.60	-0.22

Note: Bold, italic, and underlined characters represent loadings with values higher than 0.80, between 0.60 and 0.80, and between 0.40 and 0.60, respectively. ^aNine spatially resolved data and 11 time-resolved data for the Sun Metro site and 12 time-resolved data for the Sodar site were used.

coatings. The ratios of m/z 95 intensity gradually increased to 34 min and retained the plateau thereafter, and it is thought that the least volatile and high boiling point compounds making UCM are not affected by loss during several months of filter storage in SX-GC/MS analysis.

From the high degree of agreement between TD-GC/MS and SX-GC/MS, Curie-point TD-GC/MS of PM₁₀ samples collected on QF filters is a promising, fast, alternative approach to the solvent extraction-based method, which is time-consuming and uses significant quantities of harmful organic solvents. The finding of high agreement has important practical meaning for future studies in the sense that TD-GC/MS can be readily carried out on 2-hr filter samples obtained with a medium-flow (16.7 L/min) inlet and containing microgram amounts of PM, whereas SX-GC/MS method reported in the literature typically use milligram amounts of sample, for example, obtained from 24-hr filter and high-flow (1000 L/min) samples. In the final step, both the TD and SX methods use equally sensitive GC/MS analysis methods. Thus, in principle, it should be possible to perform SX-GC/MS of 2-hr filter samples as well, provided suitable microextraction methods are used. Consequently, the most important advantage of TD-GC/MS is its simplicity, speed, and lack of solvent used, thereby enabling potential use as a field-portable analysis method.

Multivariate Data Analysis

Any ambient PM sample obtained in an urban environment is likely to be a mixture of many different source components, including secondary particles. When

chromatographic and/or spectrometric methods with reasonably linear response characteristics are used, the resulting mixture profiles can (as a first approximation) be regarded as the more or less linear sums of the component profiles. Under these conditions, it is in principle possible to numerically extract the individual component profiles by means of PCA-based methods as long as the number of individual samples analyzed is substantially greater than the number of significant components present, for example, by a factor of 2 or 3.

The more dominant a relatively small number of components is, the simpler the resulting data correlation structure will be, and, consequently, the more easily the patterns of these dominant components can be extracted by PCA-based methods, though often to the detriment of smaller components. The same prominent components may be distinguishable in both space and time. This is confirmed by the high degree of correlation between the PCA results on the partially overlapping temporally and spatially resolved data sets obtained in the El Paso/Juarez airshed.

The scree plots in Figure 11 show the variation of eigenvalues of the most prominent principal components (with and without Varimax rotation) for spatially resolved, temporally resolved, and "combined" data sets. It is shown that there is a single, highly dominant first component in PCA without Varimax rotation (Figure 11a). In contrast, Varimax-rotated PCA results appear to explain each individual component more equally (Figure 11b).

The intensities of the 91 different compounds listed in Table 2 were determined by integrating the area of their key ions in the GC-MS data and used as the parameters in the matrix of PCA. Table 2 shows the first four factor

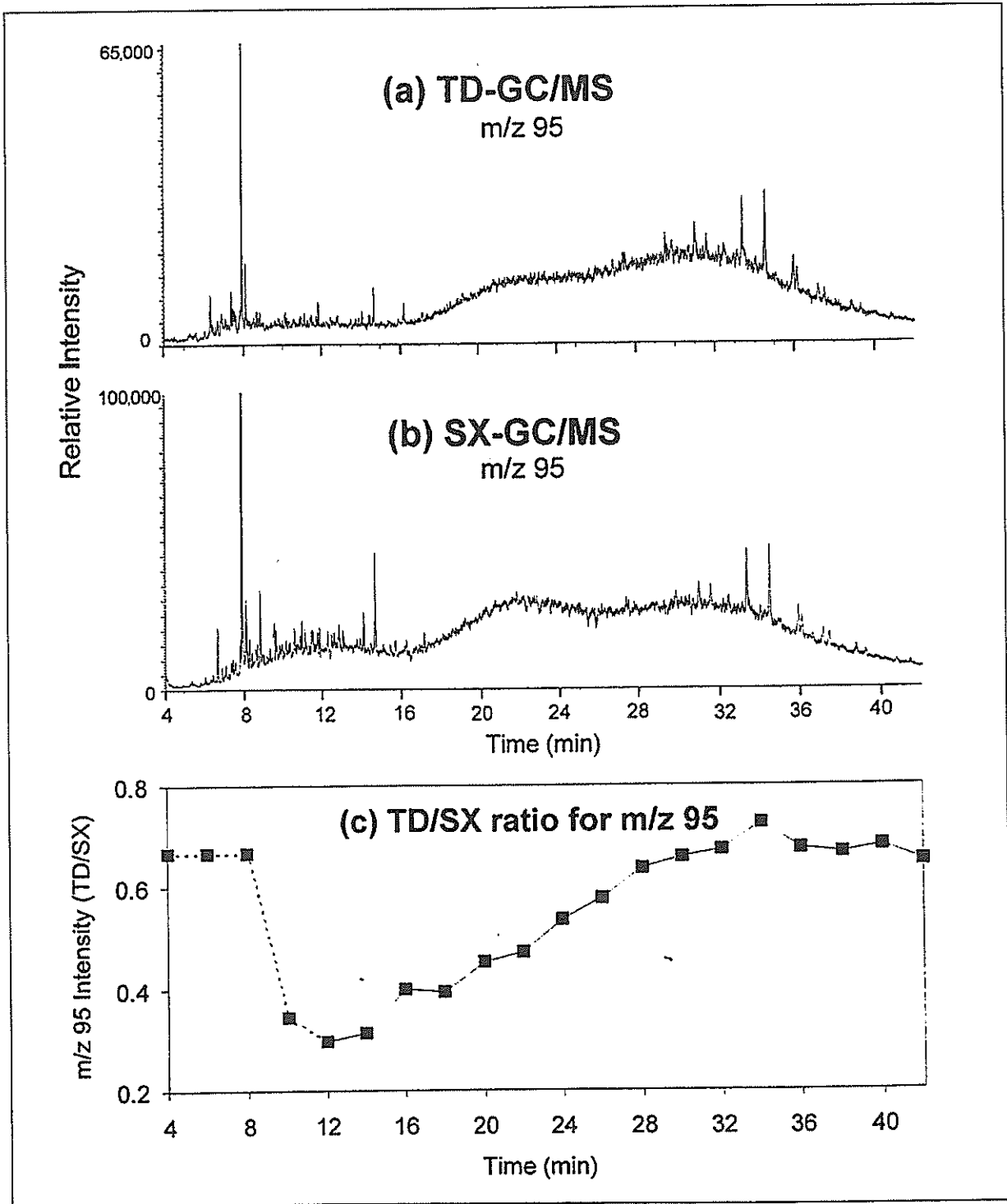


Figure 10. Ion chromatograms for m/z 95 (for naphthenes) as an indicator for the UCM in (a) TD-GC/MS and (b) SX-GC/MS, and (c) ratio of selected ion (m/z 95) between the two methods. The same data files were used for Figure 8.

loadings after Varimax rotation of the combined matrix by 23 temporally (11 for Sun Metro and 12 for Sodar sites) and 9 spatially resolved data sets with 91 compounds. These

four factors explain ~73% of the total variance in the data sets. As expected when applying the Varimax rotation technique, we can reduce intermediate strength loadings

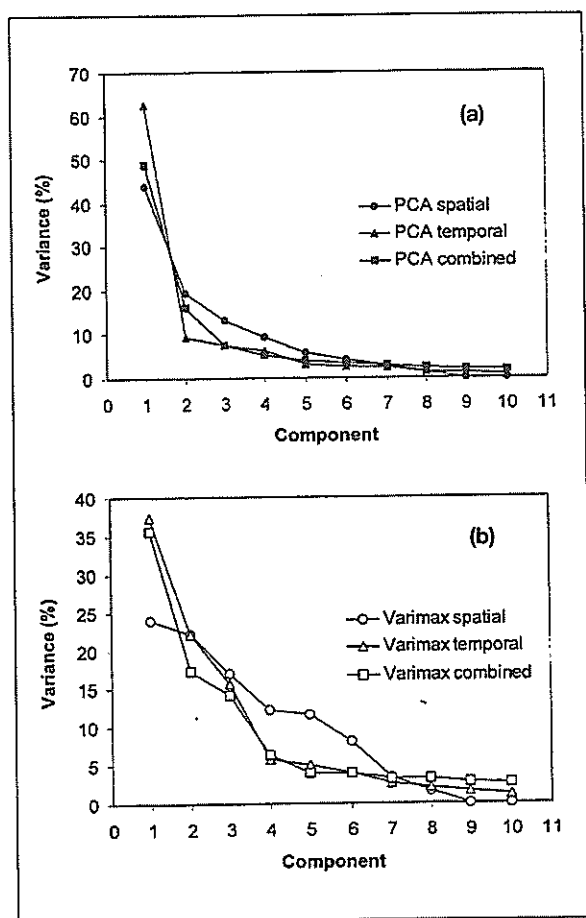


Figure 11. Variances of eigenvalues for spatially and temporally resolved and combined data sets in (a) PCA and (b) Varimax rotation. Nine spatially resolved data and 11 time-resolved data for the Sun Metro site and 12 time-resolved data for the Sodar site were used.

between 0.2 and 0.5 from the factor loadings, thereby producing prominent visible parameter association. There are highly correlated compounds with high absolute loading values found in each factor, such as hopanes and steranes, β -amyrin, and PAHs in factor 1; *n*-alkanoic acids and benzoic acid in factor 2; *n*-alkanes from tricosane to tritriacontane and some phenols in factor 3; and diethyl phthalate, some aliphatic alcohols, and phenols in factor 4.

The nature and origin of the various trends observed in the Varimax rotation can be more descriptive when factor scores are plotted as a function of time. Figure 12 shows the temporally resolved score profile for the first four prominent factors observed for the Sun Metro and Sodar sites by the TD-GC/MS method. The profiles reveal the occurrence of several strong maxima and recurring circadian rhythm in the form of one or two isolated events.

Considering highly correlated variables and the time profile in each factor shown in Table 2 and Figure 12, the PAHs, hopanes, and steranes in factor 1 reached their daily

maxima during the early morning and evening rush hours, and were thus obviously interpreted as automotive emissions. The additional extra-strength episode during the night (8:00–10:00 p.m.) of December 4 revealed the re-suspended urban dust related with the high PM concentration previously shown in Figure 4. Factor 2 shows three episodes, and two of them occurred from 12:00 to 4:00 p.m. and 6:00 to 10:00 p.m. of December 4, which also highly correlated with *n*-alkanoic acids. Thus, factor 2 is considered as biomass combustion (e.g., cooking, burning). Another episode (factor 3), which occurred early in the morning (2:00–6:00 a.m.) of December 4, does not coincide with cooking time and is thus considered a different type of PM source. The midnight episode (10:00 p.m.–2:00 a.m.) found in factor 4 is interpreted as burning products from synthetics (e.g., plasticizers), wood, and waste, indicated by the high correlation with diethyl phthalate and wood markers and phenols.

Figure 13 shows the spatially resolved score profile for four of the most significant factors for the nine Hi-Vol sampling sites, analyzed by the SX-GC/MS method, and corresponding to the factor loadings listed in Table 2. Correlation of time-resolved TD-GC/MS data with SX-GC/MS data on spatially distributed PM samples indicates a brief episode of high amyryl and long-chain *n*-alkane levels observed at the Lindbergh site. This is the location with the highest score for factor 3, and it represents PM contributions from the surrounding natural vegetation and agricultural area. Furthermore, factor 1, representing automotive emissions, is most strongly expressed in the 24-hr samples obtained at the Hi-Vol sites near the border crossings. Finally, the strong alkanolic acid, alcohol, and ketone signals seen in the 24-hr filter sample from the Advanced Transformer site, which has the highest score in factor 2, close to a major cluster of brick kilns on the southwest side of Juarez, appear to be reflected in several transient events observed at the Sun Metro and Sodar sites on the U.S. side of the border.

Therefore, from the multivariate analysis of the combined data set (Table 2 and Figures 9 and 10), the dominant four factors for PM emission sources were found to correspond to vehicular emissions plus urban dust in factor 1, biomass combustion related to cooking plus brick kilns in factor 2, native vegetation and agricultural debris in factor 3, and biomass combustion related to waste burning or firewood in factor 4. It follows from these considerations that it should be possible to use statistical correlations between temporally and spatially resolved data sets to obtain approximate source locations for observed transient or cyclical PM pollution events and, conversely, to obtain circadian activity profiles for known, prominent source types, provided both the temporal resolution and the spatial resolution in the data sets are

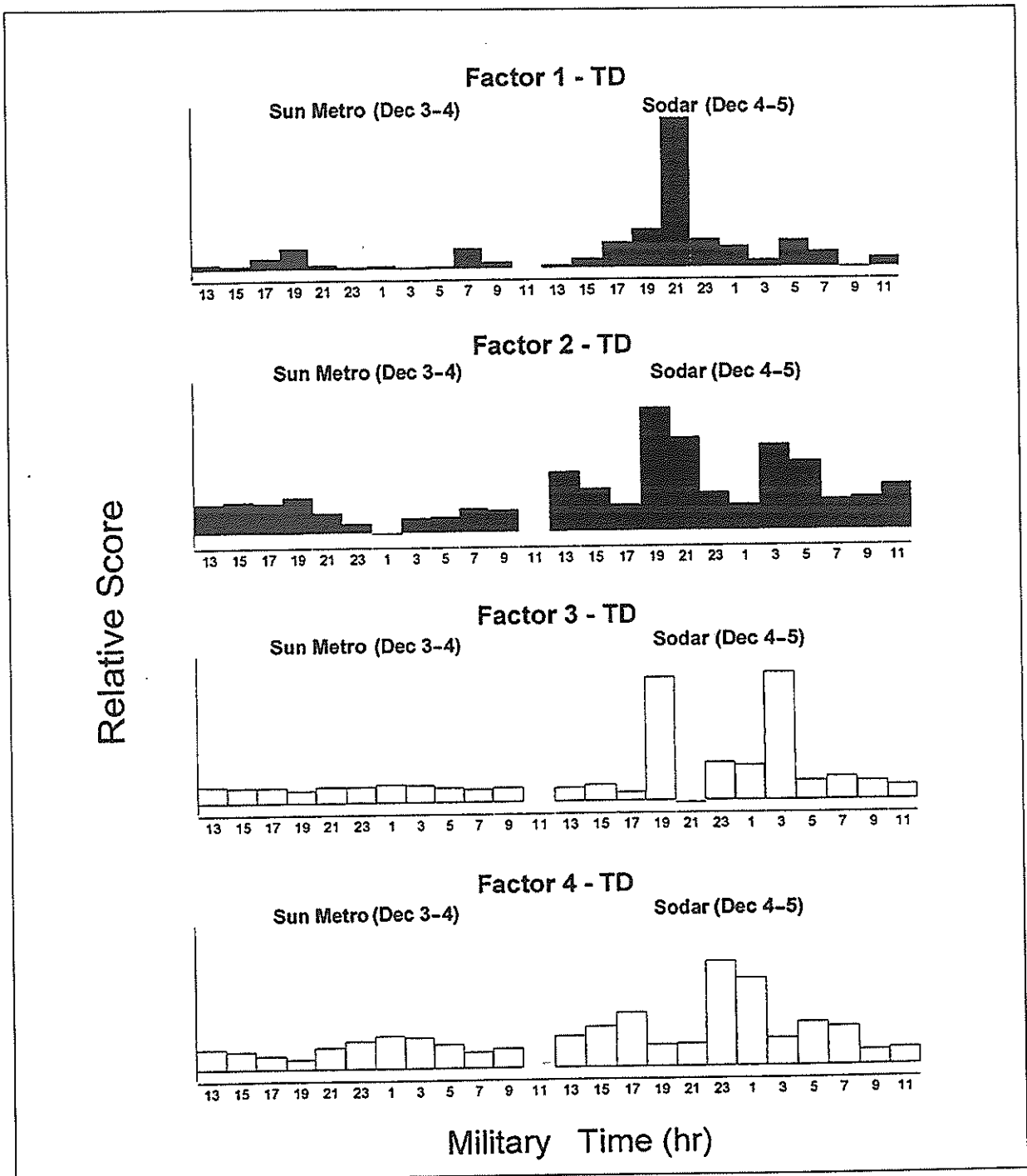


Figure 12. Time-resolved plot of factor scores for the four most significant factors in the combined data sets used in Table 2. For a complete list of chemical compounds and corresponding factor loadings, see Table 2.

adequate. In our experience, adequate temporal resolution can usually be achieved by sampling at 1-2 hourly intervals. The minimally required spatial resolution is likely to be a direct function of the complexity of the local source distributions and the variability in meteorological

conditions. Both temporally and spatially distributed sample series also need to contain a sufficiently large number of individual samples to allow the calculation of statistically meaningful correlation coefficients (i.e., preferably more than 10 or so), as well as to fulfill the

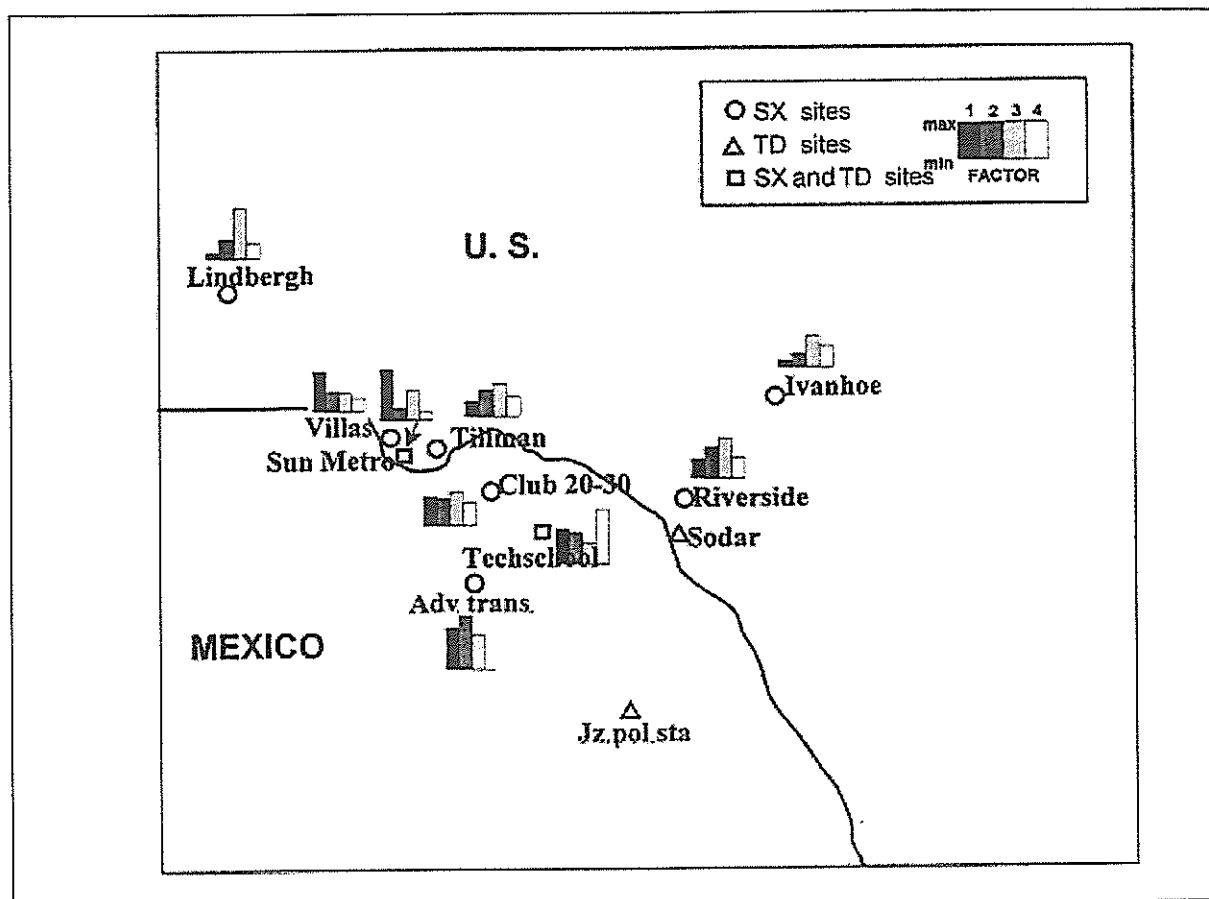


Figure 13. Spatially resolved factor scores showing the relative contributions of the four most significant factors for the nine Hi-Vol sampling sites. For a complete list of chemical compounds and corresponding factor loadings, see Table 2.

earlier mentioned requirement of a 2:1 to 3:1 ratio of samples to numerically extractable components.

CONCLUSIONS

Time-resolved PM receptor profiles obtained by 2-hr TD-GC/MS analysis were used and correlated with conventional 24-hr SX-GC/MS data on spatially resolved Hi-Vol samples to help detect and characterize sources in complex urban environments. It is concluded that

- TD-GC/MS analysis can be performed directly on small sections of QF filters loaded with microgram quantities of PM;
- The main suites of desorbed organic compounds produce TD-GC/MS profiles that are similar to those observed by conventional SX-GC/MS analysis;
- The speed of TD-GC/MS enables time-series analysis of filter samples collected at 1–2 hr intervals, thereby providing important information about transient events, such as those due to circadian anthropogenic activity cycles;
- PCA, with or without subsequent matrix rotation, of GC/MS data from temporally and spatially distributed sample series permits deconvolution of overlapping events, trends, and gradients followed by numerical extraction of characteristic component patterns;
- Numerically extracted component patterns can often be interpreted in terms of potential origins and source types, such as vehicular emissions, biomass combustion, waste burning, or plant debris;
- Systematic comparisons between GC/MS data on temporally and spatially distributed PM samples from the same airshed by means of multivariate statistical correlation methods can yield important information about the approximate source location of transient events, as well as about the circadian activity profiles of specific source types; and
- TD-GC/MS and SX-GC/MS profiles of organic PM obtained in the El Paso/Juarez airshed during a

3-day scoping study performed in December 1998 are dominated by compound suites believed to be characteristic for vehicular exhaust emissions, resuspended urban dust, biomass combustion, waste burning, and plant debris.

Since heterogeneous, poorly accessible PM sources prevent systematic sampling and characterization of individual point sources, a more efficient way to profile these sources is to sample emissions directly downwind of area sources. A new source-proximity gradient sampling approach is being tested in which dense clusters of similar sources are profiled by comparing 2-hr downwind and upwind samples to achieve the goal of source apportionment.

ACKNOWLEDGMENTS

This work has been supported by the Southwest Center for Environmental Research and Policy (SCERP; Project No.: AQ95-10) with the sponsorship of the U.S. Environmental Protection Agency and the State of Utah. We also acknowledge the invaluable help and advice of Victor Valenzuela, Gerardo Mejia, Miguel Zavala, Jacek Dworzanski, and Paul Cole.

REFERENCES

1. Rogge, W.F.; Hildemann, L.M.; Mazurek, M.A.; Cass, G.R.; Simoneit, B.R.T. *Environ. Sci. Technol.* 1991, 25, 1112-1125.
2. Rogge, W.F.; Hildemann, L.M.; Mazurek, M.A.; Cass, G.R.; Simoneit, B.R.T. *Environ. Sci. Technol.* 1993, 27, 636-651.
3. Rogge, W.F.; Hildemann, L.M.; Mazurek, M.A.; Cass, G.R.; Simoneit, B.R.T. *Environ. Sci. Technol.* 1993, 27, 1892-1904.
4. Rogge, W.F.; Hildemann, L.M.; Mazurek, M.A.; Cass, G.R.; Simoneit, B.R.T. *Environ. Sci. Technol.* 1993, 27, 2700-2711.
5. Rogge, W.F.; Hildemann, L.M.; Mazurek, M.A.; Cass, G.R.; Simoneit, B.R.T. *Environ. Sci. Technol.* 1993, 27, 2736-2744.
6. Rogge, W.F.; Hildemann, L.M.; Mazurek, M.A.; Cass, G.R.; Simoneit, B.R.T. *Environ. Sci. Technol.* 1994, 28, 1375-1388.
7. Rogge, W.F.; Hildemann, L.M.; Mazurek, M.A.; Cass, G.R.; Simoneit, B.R.T. *Environ. Sci. Technol.* 1997, 31, 2726-2730.
8. Rogge, W.F.; Hildemann, L.M.; Mazurek, M.A.; Cass, G.R.; Simoneit, B.R.T. *Environ. Sci. Technol.* 1997, 31, 2731-2737.
9. Rogge, W.F.; Hildemann, L.M.; Mazurek, M.A.; Cass, G.R.; Simoneit, B.R.T. *Environ. Sci. Technol.* 1998, 32, 13-22.
10. Schauer, J.J.; Kleeman, M.J.; Cass, G.R.; Simoneit, B.R.T. *Environ. Sci. Technol.* 1999, 33, 1566-1577.
11. Schauer, J.J.; Kleeman, M.J.; Cass, G.R.; Simoneit, B.R.T. *Environ. Sci. Technol.* 1999, 33, 1578-1587.
12. Mazurek, M.A.; Simoneit, B.R.T. In *Molecular Markers in Environmental Geochemistry*; Eganhouse, R.P., Ed.; ACS Symposium Series 671; American Chemical Society: Washington, DC, 1997; pp 92-108.
13. Simoneit, B.R.T. *J. Atmos. Chem.* 1989, 8, 251-275.
14. Simoneit, B.R.T. *Atmos. Environ.* 1984, 18, 51-67.
15. Dworzanski, J.P.; McClennen, W.H.; Cole, P.A.; Thomson, S.N.; Arnold, N.S.; Snyder, A.P.; Meuzelaar, H.L.C. *Field Anal. Chem. Technol.* 1997, 1, 295-305.

16. Voorhees, K.J.; Schulz, W.D.; Currie, L.A.; Klouda, G. *J. Anal. Appl. Pyrolysis* 1988, 14, 83-98.
17. Voorhees, K.J.; Schulz, W.D.; Kune, S.M.; Hendricks, L.J.; Currie, L.A.; Klouda, G.A. *J. Anal. Appl. Pyrolysis* 1991, 18, 189-205.
18. Dworzanski, J.P.; Berwald, L.; Meuzelaar, H.L.C. *Appl. Environ. Microbiol.* 1990, 56, 1717-1724.
19. Javitz, H.S.; Watson, J.G.; Guertin, J.P.; Mueller, P.K. *J. Air Pollut. Control Assoc.* 1988, 38, 661-667.
20. Rogge, W.F.; Hildemann, L.M.; Mazurek, M.A.; Cass, G.R.; Simoneit, B.R.T. *J. Geophys. Res.* 1996, 101, 19379-19394.
21. Rogge, W.F.; Mazurek, M.A.; Hildemann, L.M.; Cass, G.R.; Simoneit, B.R.T. *Atmos. Environ.* 1996, 27, 1309-1330.
22. Schauer, J.J.; Rogge, W.F.; Hildemann, L.M.; Mazurek, M.A.; Cass, R.C.; Simoneit, B.R.T. *Atmos. Environ.* 1996, 30, 3837-3855.
23. Hopke, P.K. *Receptor Modeling for Air Quality Management*; Elsevier Science: Amsterdam, Netherlands, 1996.
24. Windig, W.; Chakravarty, T.; Richards, J.M.; Meuzelaar, H.L.C. *Anal. Chim. Acta* 1986, 191, 205-218.
25. Cattel, R.B. *Multivariate Behav. Res.* 1966, 1, 245-251.
26. Johnson, R.A.; Wichern, D.W. *Applied Multivariate Statistical Analysis*, Prentice Hall: Upper Saddle River, NJ, 1997.
27. Mejia-Velazquez, G.M.; Meuzelaar, H.L.C. *Characterization and Dynamics of Air Pollutants in the Southeastern Mexico-U.S. Border Area*; Southwest Center for Environmental Research and Policy (SCERP) Report AQ95-10; 1997.
28. Waterman, D.; Horsfield, B.; Leistner, F.; Hall, K.; Smith, S. *Anal. Chem.* 2000, 72, 3563-3567.

About the Authors

Henk L.C. Meuzelaar (corresponding author; e-mail: meuzelaar@mail.marc.utah.edu) is a director of the Center for Micro Analysis and Reaction Chemistry (MARC) and also a professor in the Chemical and Fuels Engineering Department at the University of Utah (U of U). Sun Joo Jeon and Sue Anne N. Sheya are researchers at MARC. JoAnn S. Lighty and Adel F. Sarofim are professors in the Chemical and Fuels Engineering Department at U of U. Walter M. Jarman is a research professor and Christian Kasteler is a researcher in the Energy and Geoscience Institute at U of U. Bernd R.T. Simoneit is a professor in the College of Oceanic and Atmospheric Sciences at Oregon State University.